Article

Discovery Medicine 2025; 37(197): 1117–1129
https://doi.org/10.24976/Discov.Med.202537197.99

S100A8 Mediates Autophagy and Apoptosis in Ovarian Cancer Cells via the PI3K/Akt Pathway

Xiaojie Ma[1], Yu Wu[2], Guanyu Cao[1,*]

[1]Department of Gynaecology, Tongxiang First People's Hospital, 314500 Tongxiang, Zhejiang, China
[2]Department of Obstetrics, Tongxiang Maternal and Child Health Care Hospital, 314500 Tongxiang, Zhejiang, China
*Correspondence: 18805830125@163.com (Guanyu Cao)
Published: 9 June 2025

Background: Ovarian cancer (OC) is one of the most lethal forms of gynecological malignancies. Previous studies indicate that S100 calcium-binding protein A8 (S100A8) regulation of the phosphoinositide 3-kinase/protein kinase B (PI3K/Akt) pathway has been implicated in the development and progression of a variety of cancers, but its effects and mechanisms in OC cells remain unclear. This study aims to explore the effect of S100A8 on autophagy and apoptosis in OC cells and the regulatory effects of the PI3K/Akt signaling pathway.

Methods: Viability of OC cells was assessed by means of the 3-(4,5-dimethylthiazol-2-yl)-2,5-diphenyltetrazolium bromide (MTT) assay. Cell migration was determined using the Transwell assay. The effect of S100A8 on autophagy in OC cells was assessed using immunofluorescence and transmission electron microscopy. Flow cytometry analysis was conducted to assess apoptosis. To study the expression of genes associated with cell viability, migration, autophagy, apoptosis, and the PI3K/Akt signaling pathway, reverse transcription quantitative polymerase chain reaction (RT-qPCR) and Western blotting were performed.

Results: High concentrations of S100A8 protein significantly inhibited the activity of OC cells, with the most pronounced effect observed at 72 hours ($p < 0.05$). S100A8 protein inhibited the proliferation of OC cells and decreased the expression level of migration-driving factors ($p < 0.05$). S100A8 protein promoted apoptosis and inhibited the protein levels of Beclin 1 and microtubule-associated protein 1 light chain 3-II (LC3-II) in OC cells ($p < 0.05$). However, the PI3K/Akt activator blocked the inhibitory effects of S100A8 on OC cell activity, autophagy, and migration, and hindered it from promoting apoptosis.

Conclusions: With its ability to inhibit proliferation, migration, and autophagy, and promote apoptosis in OC cells by inhibiting the PI3K/Akt pathway, S100A8 holds promise as a potential target for the prevention and treatment of OC, providing an effective therapeutic strategy for the clinic.

Keywords: S100A8; ovarian cancer; PI3K/Akt; autophagy; apoptosis

Introduction

Ovarian cancer (OC) represents one of the most prevalent gynecological malignancies globally and is a typical heterogeneous disease. Primarily, it is categorized into three types according to the origin of the cells: germ cell carcinoma, epithelial carcinoma, and stromal carcinoma. Each type exhibits unique biological and clinical features [1,2]. Because specific symptoms and effective biomarkers are absent, about 75% of patients are diagnosed at an advanced stage (stages III and IV), where the five-year survival rate falls below 30% [3,4]. Despite the efficacy of cytoreductive surgery and platinum-based chemotherapy, most patients eventually develop resistance and experience a recurrence of the disease [5]. Therefore, identifying biomarkers and elucidating potential mechanisms are important topics in OC research.

Identified in 1965, the S100 protein family represents the most extensive subgroup among EF-hand calcium-binding proteins, comprising a total of 21 distinct members [6]. S100 proteins can function as intracellular calcium sensors as well as extracellular signaling molecules [7]. S100 calcium-binding protein A8 (S100A8) is a significant member of the S100 calcium-binding protein family, whose gene clusters in the chromosomal region 1q21, which is often deleted, translocated, or amplified in tumors, indicating its potential relationship to malignancies [7,8]. S100A8 is an inflammatory factor that participates in the inflammatory process by triggering signaling pathways through binding to cell surface receptors, playing a key role in various tumors such as colorectal cancer [9] and prostate cancer [10]. Research has shown that S100A8 is expressed not only in cancer cells but also in infiltrating immune cells and myeloid cells [11]. Furthermore, an elevated expression of S100A8 has been linked to adverse outcomes in patients suffering from breast and bladder cancers [12]. S100A8 has been confirmed to play a role in various signaling pathways, including phosphoinositide 3-kinase/protein kinase B (PI3K/Akt) [13] and p38 mitogen-activated protein kinase (p38/MAPK) [14]. S100A8 was

also found to elevate the overall levels of β-catenin and stimulate the transcription of its target genes, cellular myelocytomatosis oncogene (*c-myc*) and matrix metallopeptidase 7 (*MMP7*), leading to the activation of the Wnt/β-catenin pathway [15]. In chronic inflammatory conditions like tumors, the inflammatory proteins S100A8 and S100 calcium-binding protein A9 (S100A9) are closely associated with autophagy and apoptosis. They can enter cardiomyocytes or other cardiac cells through Toll-like receptor 4 (TLR4), bind to guanine nucleotide exchange factors (GEFs), and convert Rac family small GTPase 1/2 (Rac1/2) into their active forms as Ras homologous (Rho) guanosine triphosphatases (GTPases), thereby acting on the mechanistic target of rapamycin (mTOR) signaling pathway or the nuclear factor kappa B (NF-κB) signaling pathway to influence tumor cell migration and survival [16,17]. The study showed that the impacts of S100A8 vary across different tumors and organs, suggesting a dual role for S100A8 [18]. Notably, previous study identified S100A8 as an oocyte-expressed chemokine that functions by directing ovarian somatic cell migration [19]. In addition, S100A8 protein is a unique salivary protein marker for non-invasive OC diagnosis [1]. However, the effect and mechanisms of S100A8 on OC cells remain unclear. Hence, this study aims to explore the impacts and mechanisms of S100A8 on autophagy and apoptosis in OC cells.

The PI3K/Akt signaling cascade plays an essential role in promoting oncogenic activities [20]. Akt, a vital signaling molecule, phosphorylates several downstream targets, connecting them to multiple interrelated signaling pathways. Upon receiving signals, PI3K attaches to cell membrane receptors, which activate Akt. Akt then moves to the cell membrane to gain catalytic activity, subsequently regulating downstream effector proteins [21]. The PI3K/Akt signaling cascade is involved in the regulation of multiple cellular functions, including cell cycle progression, cell survival, cell migration, autophagy, and apoptosis [22–26]. Akt is recognized for its overexpression in various human cancers and is linked with unfavorable prognosis in some types of cancer [27]. Thus, it is speculated that the PI3K/Akt pathway may play a role in the advancement of OC.

In the present study, we found that S100A8 is an anti-oncogene that may inhibit OC cell proliferation, migration, and autophagy, and promote apoptosis by suppressing the PI3K/Akt pathway.

Materials and Methods

Cell Culture and Treatment

Human OC cell lines 3AO (mucinous; YB-H0141) were purchased from the Shanghai Ybscience Technology Co., Ltd. (Shanghai, China), whereas SKOV3 (serous; SCSP-5214) was purchased from the Shanghai Cell Bank of the Chinese Academy of Sciences (Shanghai, China). All cell lines were validated with short tandem repeat (STR) profiling and were found to be free of mycoplasma contamination. The 3AO and SKOV3 cells, once frozen, were quickly thawed in a water bath at 37 °C, centrifuged at 3000 rpm for 10 minutes, and the supernatant was subsequently discarded. Then, the cell pellet was resuspended in Roswell Park Memorial Institute 1640 (RPMI-1640) (11875119, Thermo Fisher Scientific, Waltham, MA, USA) culture medium enriched with 10% fetal bovine serum (FBS) and incubated at 37 °C within an incubator maintaining a 5% CO_2 atmosphere. A series of six S100A8 concentrations—0, 2, 4, 6, 8, and 16 µmol/L—were subjected to a preliminary concentration gradient screening to determine the best concentration for the subsequent experiments. Based on previous studies, 1,5-dicaffeoylquinic acid (1,5-DQA) (B28155, Shanghai Yuanye Bio-Technology Co., Ltd., Shanghai, China), a PI3K/Akt activator, was selected for use in the experiment [28]. Both 3AO and SKOV3 cells were exposed to varying concentrations of S100A8 protein (0, 2, 4, 6, 8, 16 µmol/L) (ZY792Bo011, HZbscience, Shanghai, China) and 1,5-DQA (50 µmol/L, B28155, Shanghai Yuanye Bio-Technology Co., Ltd., Shanghai, China).

The groups in this study were as follows: 0 µmol/L group, no exogenous S100A8 was added; 2 µmol/L group, added 2 µmol/L of S100A8; 4 µmol/L group, added 4 µmol/L of S100A8; 6 µmol/L group, added 6 µmol/L of S100A8; 8 µmol/L group, added 8 µmol/L of S100A8; 16 µmol/L group, added 16 µmol/L of S100A8; Blank group, no exogenous S100A8 was added; S100A8 group, added 16 µmol/L of S100A8; S100A8+1,5-DQA group, on the basis of 16 µmol/L S100A8, 50 µmol/L PI3K/Akt activator 1,5-DQA was added.

MTT Assay

Cells from each treatment group were collected and adjusted to a density of 5×10^3 cells/mL, then plated into a 96-well plate and maintained in a 37 °C, 5% CO_2 incubator. After culturing for periods of 24, 48, and 72 hours, each well received 20 µL of a 5 g/L 3-(4,5-dimethylthiazol-2-yl)-2,5-diphenyltetrazolium bromide (MTT) reagent (BTM-30006, Biotium, Fremont, CA, USA). Subsequently, the wells were incubated in the dark for 4 hours. Afterwards, the culture was terminated and the supernatant removed. Then, 200 µL of dimethyl sulfoxide (DMSO) (D2650, Sigma-Aldrich, St. Louis, MO, USA) solution was introduced to each well. This was followed by shaking to ensure complete dissolution of the crystals. Using a microplate reader (MODEL680, Bio-Rad, Hercules, CA, USA), the optical density (OD) of each well was assessed at a wavelength of 490 nm. The cell viability was determined by using the following formula: Cell viability (%) = (OD of experimental group – OD of blank group)/(OD of control group – OD of blank group) $\times$ 100.

Table 1. Sequence of RT-qPCR primers.

Gene	Forward (5′–3′)	Reverse (5′–3′)
Ki67	CACGAGACGCCTGGTTACTA	AGTTGGGTCTCCCCCTGTAA
PCNA	TGTTGGAGGCACTCAAGGAC	GAGTCCATGCTCTGCAGGTT
MMP2	TGATGGCATCGCTCAGATCC	GGCCTCGTATACCGCATCAA
MMP7	GGAGTGCCAGATGTTGCAGA	ATCTCCTCCGAGACCTGTCC
MMP9	TCTATGGTCCTCGCCCTGAA	CATCGTCCACCGGACTCAAA
Bax	CGGGGAGCAGCCCAGAG	GTCTTGGATCCAGCCCAACA
Caspase 3	TGCTATTGTGAGGCGGTTGT	TTCCCTGAGGTTTGCTGCAT
Bcl-2	ACAGGGTACGATAACCGGGA	CAATCCTCCCCCAGTTCACC
β-Actin	TCGAGGCTTTCAACACACCA	GATCCAGGCGTAGAATGGCA

RT-qPCR, reverse transcription quantitative polymerase chain reaction; *Ki67*, ki67 antigen; *PCNA*, proliferating cell nuclear antigen; *MMP2*, matrix metallopeptidase 2; *MMP7*, matrix metallopeptidase 7; *MMP9*, matrix metallopeptidase 9; *Bax*, Bcl-2-associated x protein; *Caspase 3*, cysteine-aspartic acid protease 3; *Bcl-2*, B-cell lymphoma 2; *β-Actin*, beta-actin.

Quantitative Reverse Transcription Polymerase Chain Reaction

Total RNA was isolated from the cells using TRIzol (15596026, Invitrogen, Mountain View, CA, USA) and confirmed for purity and concentration using a ultraviolet-visible (UV-visible) spectrophotometer (752, INESA, Shanghai, China). The extracted total RNA was subsequently converted into complementary DNA (cDNA) through reverse transcription using Hifair II 1st Strand cDNA Synthesis Kit (11119ES60, Yeasen, Shanghai, China) and conducted under the following conditions: 42 °C for 60 minutes and 72 °C for 5 minutes. The total RNA extracted was subsequently reverse-transcribed into cDNA under specific conditions: 42 °C for 55 minutes, followed by 72 °C for 5 minutes. Table 1 lists sequences of primers used in this study. Then, the reverse transcription quantitative polymerase chain reaction (RT-qPCR) was performed on a Bio-Rad QuantStudioTM Real-Time System (Thermo Fisher Scientific, Waltham, MA, USA) using the RT-qPCR kit (RR071A, BIOSCIENCE, Hong Kong, China) in accordance with the manufacturer's instructions. The reaction conditions were: 95 °C for 5 minutes, followed by 38 cycles of 95 °C for 7 seconds, 60 °C for 30 seconds, and 65 °C for 35 seconds. The PCR experiments were repeated three times with three replicate wells each time, the relative expression levels were measured using the $2^{-\Delta\Delta CT}$ method.

Western Blotting

Cells from each treatment group were collected, and radioimmunoprecipitation assay (RIPA) lysis buffer containing phenylmethanesulfonyl fluoride (PMSF) was added to extract the total protein. The extracted protein was quantified using the bicinchoninic acid (BCA) method, ensuring that it met quality standards. Equal volumes of sample loading buffer were added, and the samples were heated in a 100 °C water bath for 5 minutes to completely denature the proteins. Twenty micrograms of denatured protein were subjected to separation via sodium dodecyl sulfate polyacrylamide gel electrophoresis (SDS-PAGE). After electrophoresis, the protein products were transferred to a polyvinylidene difluoride (PVDF) membrane. The membrane was treated at ambient temperature for 60 minutes with 5% nonfat dry milk to block nonspecific binding sites. Following this, the membrane was incubated with primary antibodies overnight at 4 °C, as follows: anti-ki67 antigen (Ki67) (1:1000, ab16667, Abcam, Cambridge, UK), anti-proliferating cell nuclear antigen (PCNA) (1:1000, ab18197, Abcam, Cambridge, UK), anti-matrix metallopeptidase 2 (MMP2) (1:2000, ab92536, Abcam, Cambridge, UK), anti-MMP7 (1:1000, ab216631, Abcam, Cambridge, UK), anti-matrix metallopeptidase 9 (MMP9) (1:1000, ab73734, Abcam, Cambridge, UK), anti-PI3K (1:2000, ab131067, Abcam, Cambridge, UK), anti-Beclin 1 (1:2000, ab62557, Abcam, Cambridge, UK), anti-microtubule-associated protein 1 light chain 3 (LC3)-II/LC3-I (1:2000, 12741, Cell Signaling Technology, Inc, Beverly, MA, USA), anti-beta-actin (β-Actin) (1:1000, ab1801, Abcam, Cambridge, UK), anti-Akt (1:1000, ab38449, Abcam, Cambridge, UK). On the subsequent day, the membrane was washed and then treated with a horseradish peroxidase-labeled immunoglobulin G (IgG) secondary antibody (ab288151, 1:2000, Abcam), followed by a 60-minute room temperature incubation. For luminescence, enhanced chemiluminescence (ECL) (32106, Pierce, Waltham, MA, USA) was utilized. Lastly, the membrane was exposed and processed in a darkroom. Photos were taken using an automatic gel imaging system (CliNX, ChemiScope 6200, Shanghai Qinxiang Scientific Instrument Co., Ltd., Shanghai, China). β-Actin served as the internal reference. The expression level of the target protein was assessed by calculating the ratio of the density values of the target protein band to those of the internal reference pro-

tein band. The analysis of these bands was performed using ImageJ software (V1.8.0.112, NIH, Madison, WI, USA).

Transwell Migration Assays

The 1.5×10^5 cells were placed into the upper chambers of a Transwell plate featuring 8 µm pores (Sigma-Aldrich, St. Louis, MO, USA). For the migration assay, the lower compartments were filled with 800 µL of RPMI-1640 supplemented with 10% fetal bovine serum (FBS) to serve as a chemoattractant. Cells that had migrated to the lower surface of the membrane were fixed using 4% paraformaldehyde for 35 minutes and subsequently stained with 0.1% crystal violet (M07174, Balb, Beijing, China) for 1 hour at room temperature. Following staining, the cells were visualized under a microscope (IX51, Olympus, Tokyo, Japan) and counted at 100× magnification.

Immunofluorescence

3AO and SKOV3 cells were grown in cell culture dishes. After fixation with precooled methanol for 20 minutes, the cells were permeabilized using 0.2% Triton X-100 in phosphate-buffered saline (PBS) for an additional 20 minutes, and then incubated with 2% bovine serum albumin in PBS to block non-specific sites for 35 minutes. Then, the cells were incubated with rabbit polyclonal p62 (1:50, ab314504, Abcam, Cambridge, UK) and mouse polyclonal microtubule-associated protein 1 light chain 3 (LC3) primary antibodies (1:50, ab244210, Abcam, Cambridge, UK) at 37 °C for 80 minutes. Subsequently, the cells were incubated with secondary antibodies, goat anti-rabbit immunoglobulin G tagged with Texas Red (IgG-TR) (1:10,000, ab6718, Abcam, Cambridge, UK) and donkey anti-mouse immunoglobulin G conjugated with fluorescein isothiocyanate (IgG-FITC) (1:10,000, ab6816, Abcam, Cambridge, UK), at 37 °C for 1 hour, and then labeled with 4′,6-diamidino-2-phenylindole (DAPI) (1:1000, ab104139, Abcam, Cambridge, UK). The images were captured using a confocal microscope (FV3000, Olympus, Tokyo, Japan) and Slidebook 4.2.0.11 computer software (Intelligent Imaging Innovations, Inc., Denver, CO, USA).

Transmission Electron Microscopy

The cells were post-fixed with 2.5% glutaraldehyde in a 0.1 M phosphate buffer for 2.5 hours at 4 °C, followed by post-fixation with 1% osmium tetroxide for 3.5 hours. Samples were collected by scraping and then centrifuged (1000 rpm/min, 4 °C, 5 min) to form pellets, which subsequently underwent dehydration through a series of successive graded ethanol solutions. After the dehydration step, the specimens were infiltrated and embedded with Epon™ resin. After sectioning procedure using a Leica Ultracut Microtome (Leica EM UC6, Leica Microsystems Inc., Buffalo Grove, IL, USA), ultrathin sections, approximately 70 nm thick, were stained with uranyl acetate for 3 minutes, and examined with a JEOL JEM-1400 transmission electron microscope (JEOL Ltd., Tokyo, Japan).

Flow Cytometry

The cells from each treatment group were collected and seeded at a density of 1×10^5 cells per well in a 6-well plate, then cultured in a 37 °C, 5% CO_2 cell incubator. After culturing for 24 hours, the cells were digested with trypsin, centrifuged (1000 rpm/min, 4 °C, 5 min), and the supernatant was discarded to collect the cell pellet. The pellet was resuspended in 200 µL of binding buffer, followed by the sequential addition of 10 µL of Annexin V-fluorescein isothiocyanate (Annexin V-FITC) (C1062L, Beyotime, Beijing, China) and 10 µL of propidium iodide (PI). The mixture was gently stirred and then left to incubate in the dark at room temperature for 15 minutes. Following this, 300 µL of binding buffer was introduced. The cells were analyzed with a flow cytometer (FC-500, Beckman, Fullerton, CA, USA), and the resulting data were processed using ImageJ (V1.8.0.112, NIH, Madison, WI, USA).

Statistical Analysis

Data processing and analysis were carried out using GraphPad Prism 8.0 software (GraphPad Software, San Diego, CA, USA), with each experiment conducted in triplicate. For comparisons involving multiple groups, one-way analysis of variance (ANOVA) followed by Tukey's post hoc test was applied, whereas differences between two groups were assessed using a *t*-test. Results are expressed as mean ± standard deviation, and results with *p*-values below 0.05 were considered statistically significant.

Results

Exogenous S100A8 Inhibited the Activity of Ovarian Cancer Cells

To examine the effect of exogenous S100A8 on the viability of OC cells, we utilized the MTT assay to treat OC cells 3AO and SKOV3 with different concentrations of S100A8 protein (0, 2, 4, 8, 16 µmol/L) for 24, 48, and 72 hours. The results showed that, compared to the 0 µmol/L group, the activity of 3AO and SKOV3 in the 16 µmol/L group was significantly reduced, and at 72 hours, it was significantly lower than at 24 hours ($p < 0.05$) (Fig. 1a,b). In addition, we also assessed the protein and mRNA levels of the proliferation markers *Ki67* and *PCNA* using RT-qPCR and Western blotting. Compared to the 0 µmol/L group, the mRNA levels of *Ki67* and *PCNA* in other S100A8 concentration groups were significantly reduced, with a pronounced effect in the 8 and 16 µmol/L groups ($p < 0.01$) (Fig. 1c–f). Similarly, the protein levels of Ki67 and PCNA in the 2, 4, 8, and 16 µmol/L groups were lower than those in the 0 µmol/L group, and more significantly in the 16 µmol/L group ($p < 0.01$) (Fig. 1g–l). Collectively, these findings indicate that exogenous S100A8 suppresses the activity of OC cells.

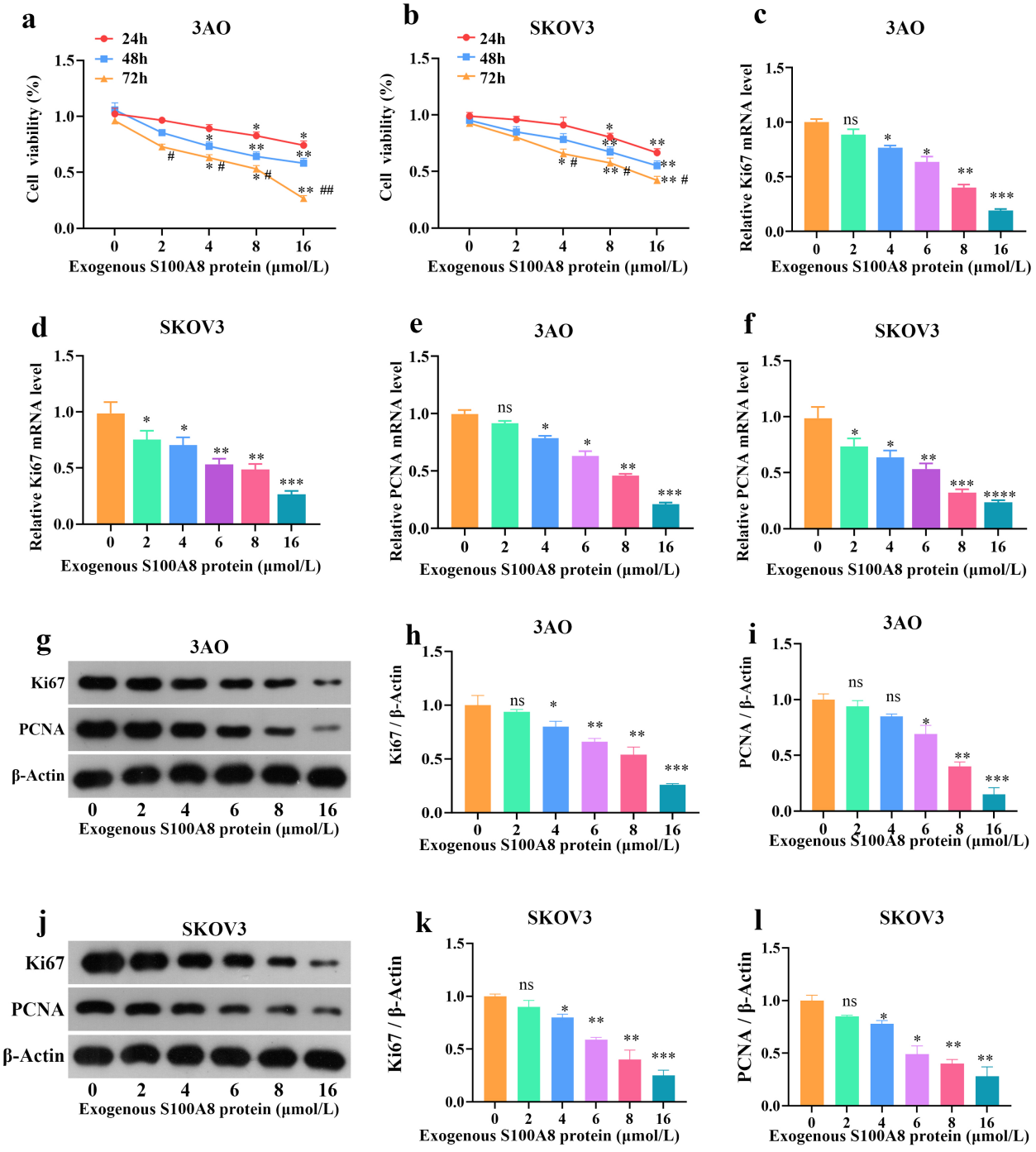

Fig. 1. Effect of exogenous S100A8 on the viability of OC cells. (a,b) Detection of 3AO and SKOV3 cells activity by means of MTT assay. (c–f) The mRNA levels of proliferation markers *Ki67* and *PCNA* were measured using RT-qPCR. (g–l) The protein levels of Ki67 and PCNA were detected by means of Western blotting. $n = 3$. $^{*}p < 0.05$, $^{**}p < 0.01$, $^{***}p < 0.001$, $^{****}p < 0.0001$ versus 0 μmol/L group; $^{\#}p < 0.05$, $^{\#\#}p < 0.01$versus 24 h group; ns, no significant difference. Abbreviations: OC, ovarian cancer; S100A8, S100 calcium-binding protein A8; MTT, 3-(4,5-dimethylthiazol-2-yl)-2,5-diphenyltetrazolium bromide.

Exogenous S100A8 Inhibited the Migration of Ovarian Cancer Cells

To determine whether exogenous S100A8 hampers the metastasis of OC cells, RT-qPCR and Western blot analyses were conducted to evaluate the expression levels of MMP2, MMP7, and MMP9, which are crucial regulatory molecules in cancer cell invasion and migration in OC. The RT-qPCR results showed that compared with the 0 μmol/L group, the mRNA levels of *MMP2*, *MMP7*, and *MMP9* were significantly reduced in the 16 μmol/L group ($p <$

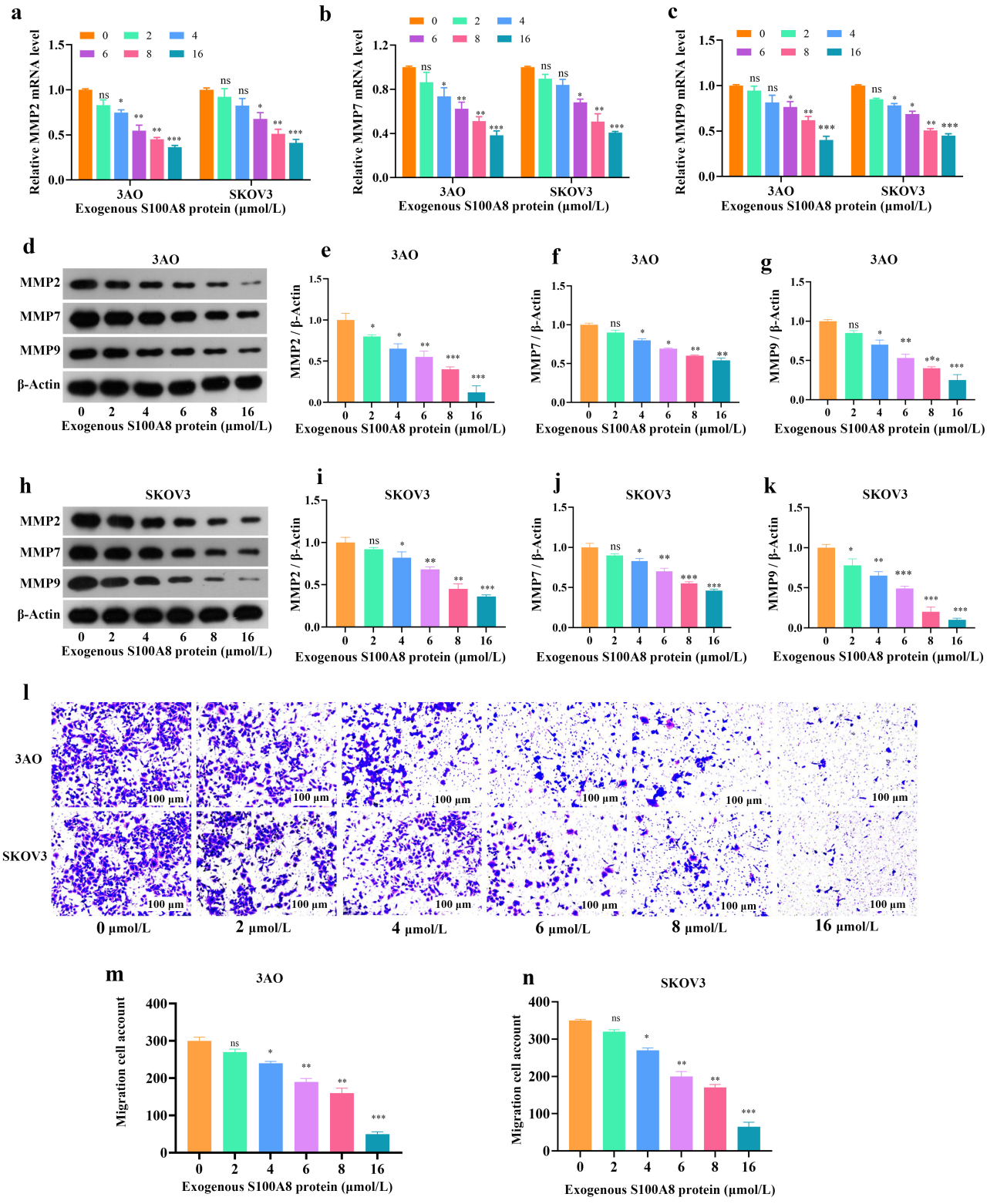

Fig. 2. Effects of exogenous S100A8 on migration of OC cells. (a–c) The mRNA levels of key factors of cancer migration were measured by RT-qPCR. (d–k) The protein levels of key factors of cancer migration were detected by Western blotting. (l–n) Migratory capacity of OC cells analyzed by Transwell assay. $n = 3$. *$p < 0.05$, ** $p < 0.01$, ***$p < 0.001$ versus 0 μmol/L group; ns, no significant difference.

0.001) (Fig. 2a–c). Western blot results indicated that the protein levels of MMP2, MMP7, and MMP9 were significantly decreased in the 16 μmol/L group compared to the 0 μmol/L group, as shown in Fig. 2d–k ($p < 0.01$). The results

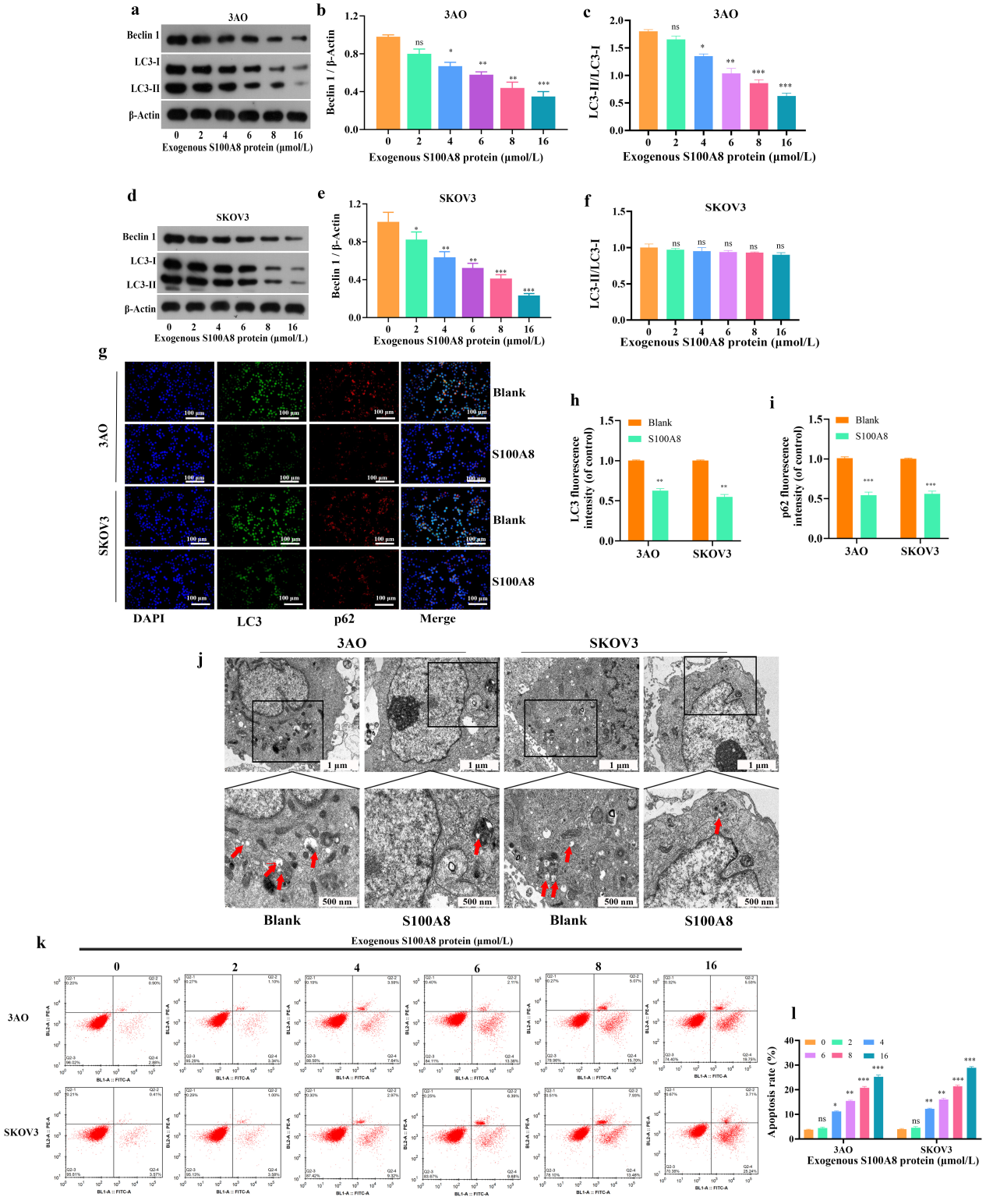

Fig. 3. Effect of exogenous S100A8 on autophagy and apoptosis in OC cells. (a–f) Autophagy-related protein Beclin 1 and microtubule-associated protein 1 light chain 3 (LC3)-II/LC3-I levels were analyzed by means of Western blotting. (g–i) Immunofluorescence staining for LC3 and p62 was conducted in 3AO and SKOV3 cell lines, with the red fluorescence indicating p62 expression and the green fluorescence corresponding to LC3 levels. (j) Electron microscopy images showing autophagosomes, as indicated by arrows. (k,l) Level of apoptosis detected through flow cytometry analysis. $n = 3$. *$p < 0.05$, **$p < 0.01$, ***$p < 0.001$ versus 0 μmol/L group; ns, no significant difference. Abbreviation: DAPI, 4′,6-diamidino-2-phenylindole.

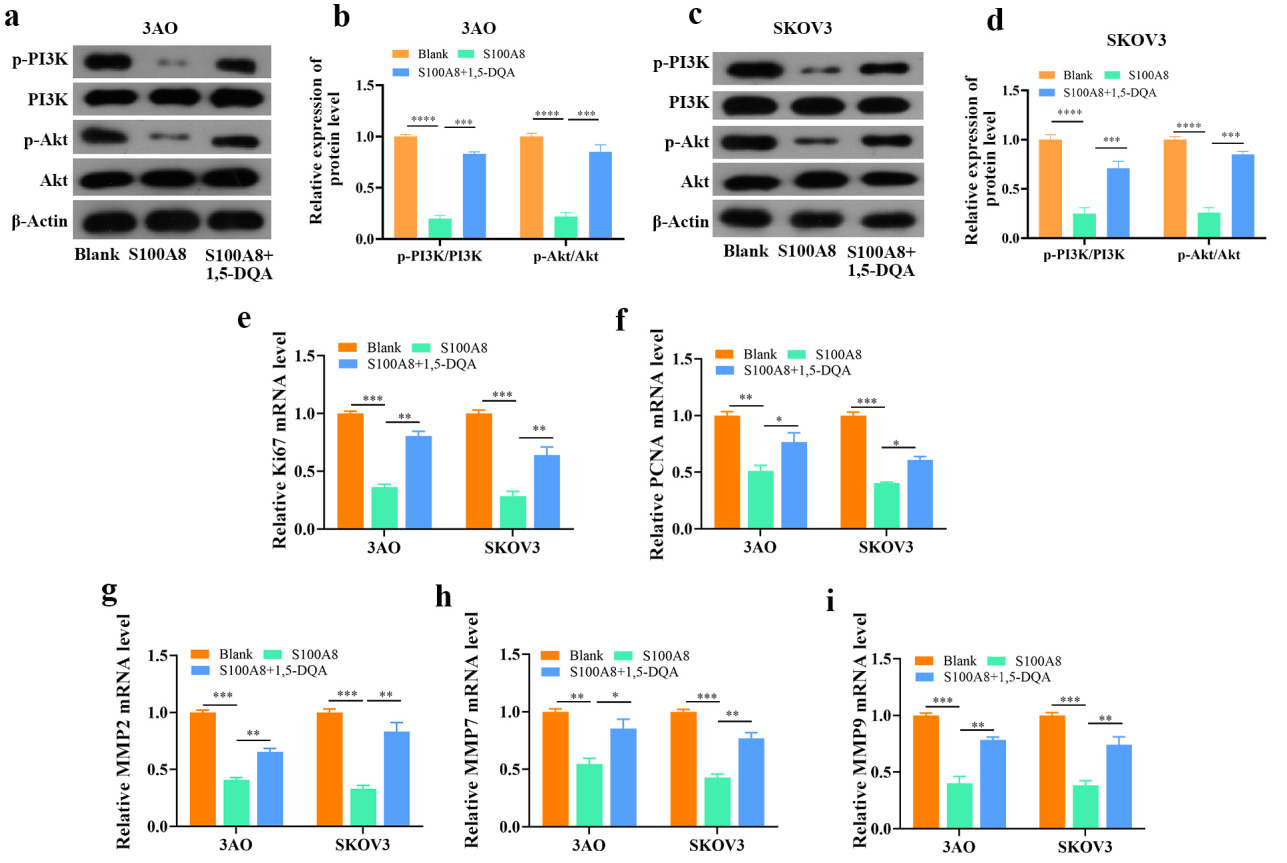

Fig. 4. PI3K/Akt blocked the effects of S100A8 on OC cell proliferation and migration. (a–d) The phosphorylation level of PI3K/Akt was detected through Western blotting. (e–i) The mRNA levels of *Ki67*, *PCNA*, *MMP2*, *MMP7* and *MMP9* detected by means of RT-qPCR. $n = 3$. *$p < 0.05$, **$p < 0.01$, ***$p < 0.001$, ****$p < 0.0001$. Abbreviations: 1,5-DQA, 1,5-Dicaffeoylquinic acid; PI3K/Akt, phosphoinositide 3-kinase/protein kinase B.

of the Transwell assay showed that the migratory ability of the two OC cells decreased as the concentration of exogenous S100A8 gradually increased ($p < 0.05$) (Fig. 2l–n). Therefore, the results show that exogenous S100A8 inhibits the migration of OC cells.

Effect of Exogenous S100A8 on Autophagy and Apoptosis in Ovarian Cancer Cells

To elucidate the impact of S100A8 on autophagy and apoptosis in OC cells, we investigated the expression of genes related to autophagy and measured the rate of apoptosis. In the 3AO cells, compared with the 0 µmol/L group, the protein level of Beclin 1 and the ratio of LC3-II/LC3-I in the 16 µmol/L group were significantly decreased ($p < 0.001$) (Fig. 3a–c). However, in SKOV3 cells, compared with the 0 µmol/L group, the protein level of Beclin 1 was significantly decreased in the 16 µmol/L group ($p < 0.001$) (Fig. 3d,e), but the LC3-II/LC3-I ratio showed no statistical difference ($p > 0.05$) (Fig. 3d–f). Immunofluorescence analysis of LC3 and p62 revealed that the autophagy level in cells significantly decreased after exogenous S100A8 intervention ($p < 0.05$) (Fig. 3g–i). Electron microscopy analysis further revealed that S100A8 treatment reduced the number of autophagosomes in both cell lines (Fig. 3j).

Furthermore, compared with the 0 µmol/L group, the apoptosis ratio of 3AO and SKOV3 cells elevated significantly in the 16 µmol/L group ($p < 0.001$) (Fig. 3k,l). The results revealed that S100A8 suppressed autophagy and boosted apoptosis in OC cells, and exerted anticancer effects. Therefore, the S100A8 concentration of 16 µmol/L was chosen for the subsequent experiments.

PI3K/Akt Blocked the Inhibitory Effect of S100A8 on Ovarian Cancer Cell Proliferation and Migration

To determine whether PI3K/Akt blocks the inhibitory effect of S100A8 on the proliferation and migration of OC cells, we treated the 3AO and SKOV3 cells with a PI3K/Akt pathway activator. Compared with the blank group, the S100A8-treated group exhibited a marked decrease in the ratios of p-PI3K/PI3K and p-Akt/Akt protein expression ($p < 0.01$). P-PI3K/PI3K and p-Akt/Akt protein levels were higher than those in the S100A8 group after PI3K/Akt activator treatment ($p < 0.05$) (Fig. 4a–d). Similarly, mRNA levels of the proliferation markers *Ki67* and *PCNA*, as well

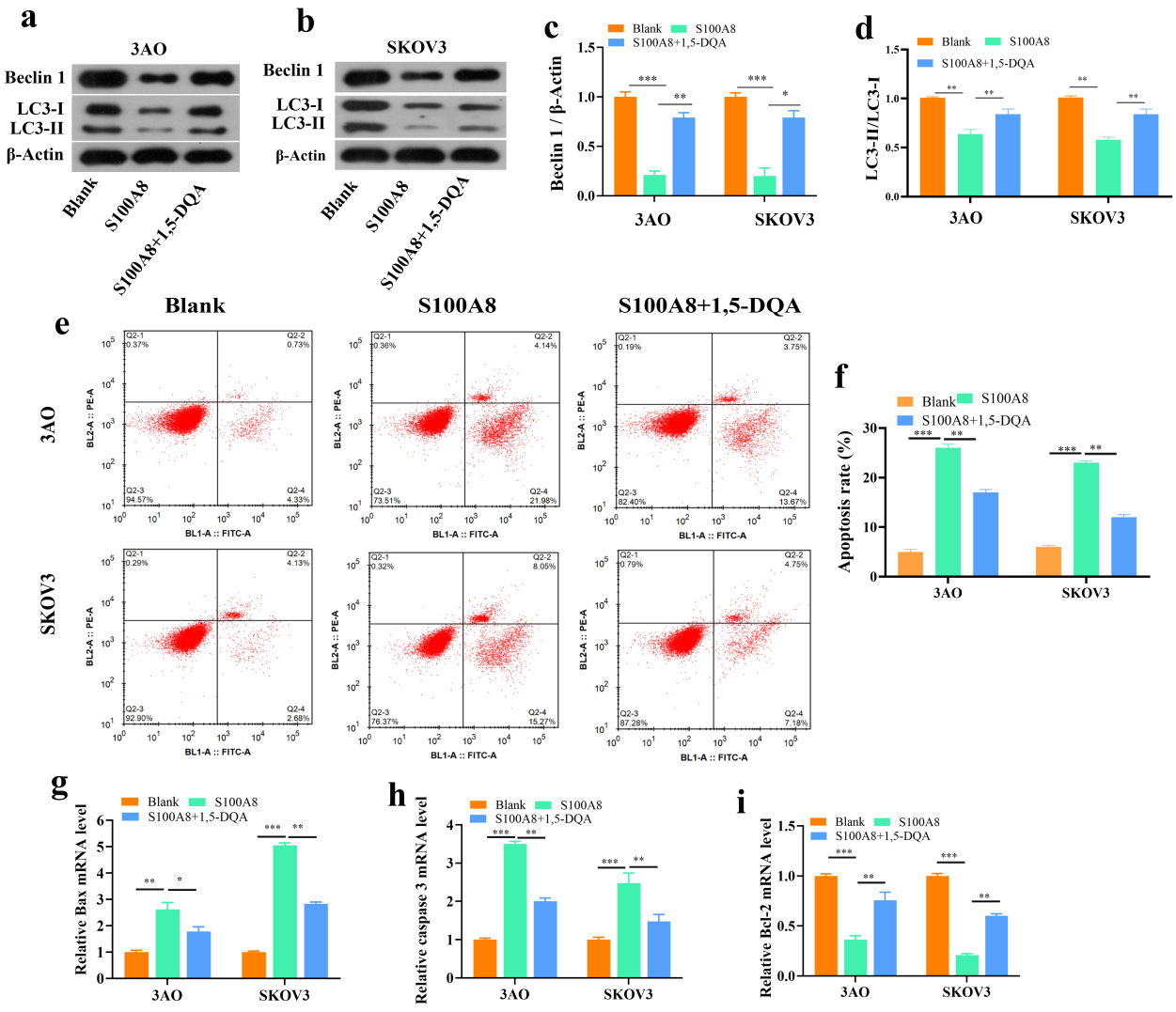

Fig. 5. PI3K/Akt blocked the effects of S100A8 on OC cell autophagy and apoptosis. (a–d) Western blot assessment of Beclin 1 and LC3-II/LC3-I protein expression. (e,f) Flow cytometry assessment of the apoptosis rate of 3AO and SKOV3 cells in each group. (g–i) The mRNA levels of apoptosis markers *Bax*, *caspase 3* and *Bcl-2* detected by RT-qPCR. $n = 3$. *$p < 0.05$, **$p < 0.01$, ***$p < 0.001$.

as the migration-regulating factors MMP2, MMP7, and MMP9, were significantly increased after PI3K/Akt activator intervention ($p < 0.05$) (Fig. 4e–i). Briefly, the results reveal that the activation of the PI3K/Akt pathway obstructs the suppressive impact of S100A8 on the proliferation and migration of OC cells.

PI3K/Akt Blocked the Effects of S100A8 on Autophagy and Apoptosis in Ovarian Cancer Cells

Compared to the blank group, LC3-II and Beclin 1 protein levels were markedly decreased in the S100A8 group ($p < 0.01$). In comparison to the S100A8 group, the protein levels of LC3-II/LC3-I and Beclin 1 in the PI3K/Akt activator group were significantly increased (Fig. 5a–d). Besides, compared with the S100A8 group, the apoptosis ratio of 3AO and SKOV3 cells was reduced significantly in the PI3K/Akt activator group ($p < 0.01$) (Fig. 5e,f). Our RT-qPCR data showed that mRNA levels of the apoptosis marker B-cell lymphoma 2 (*Bcl-2*) were significantly increased after PI3K/Akt activator intervention, whereas levels of Bcl-2-associated x protein (Bax) and caspase 3 were significantly decreased, as shown in Fig. 5g–i ($p < 0.05$). Collectively, these outcomes indicate that the activation of the PI3K/Akt pathway obstructs the influence of S100A8 on both autophagy and apoptosis in OC cells.

Discussion

Although many studies have indicated that S100A8 plays an anti-cancer role in colorectal carcinoma and thyroid cancer [29,30], its mechanisms as an anti-cancer agent remain unclear, especially in OC. In this study, high concentrations of S100A8 significantly inhibited cell proliferation, autophagy and migration, while promoting apopto-

sis. Additionally, the PI3K/Akt pathway blocked the effects of S100A8 on the proliferation, migration, autophagy, and apoptosis of OC cells. Previous studies have also found similar results [31,32]. The results of this study establish a theoretical foundation for identifying biomarkers and understanding the potential mechanisms of OC, which could contribute to lowering the mortality rate among women affected by this disease.

The *S100A8* gene is located at the chromosome locus 1q21.3. Dimova *et al*. [33] reported that amplification at this locus occurs in ovarian cancers. Dysregulation of S100A8 expression is commonly observed in various cancers and is linked to tumorigenesis and progression in cancers, including breast cancer [34], colorectal cancer [35], and kidney cancer [36]. Furthermore, an association exists between S100A8 and poor prognosis in patients with bladder cancer [12]. Additional research has demonstrated that extracellular S100A8/S100A9 promotes a potent anti-tumor response by enhancing cytotoxicity and inducing apoptosis [37]. However, there is currently limited research on the effects of S100A8 on OC and its potential molecular mechanisms. In this study, the S100A8 protein markedly decreased the viability and restricted the migration of OC cells. These results align with prior studies conducted on thyroid cancer [30] and colorectal carcinoma [29].

Autophagy and apoptosis are recognized as crucial pathways that contribute to various human diseases, including cancer, inflammatory conditions, and heart failure [38,39]. Beclin 1, an autophagy-related protein, participates in tumorigenesis and progression by influencing the cell cycle, regulating tumor cell apoptosis, and modulating tumor angiogenesis [40,41]. The LC3 protein is predominantly located on the surfaces of autophagosomes and autophagic membranes, where it plays a key role in autophagosome formation [42]. In this study, S100A8 was found to reduce the expression levels of Beclin1, LC3 II and p62, and the number of autophagosomes in OC cells, consistent with previous findings in tumors such as cervical cancer [43] and pancreatic cancer [44]. Furthermore, another report indicates that S100A8/S100A9 demonstrates a robust anti-tumor response by enhancing apoptosis [37], aligning with the findings of this study. Li *et al*. [45] also confirmed the relationship between autophagy and apoptosis: blockade of autophagy by 3-methyladenine increased apoptosis. However, in acute myeloid leukemia, S100A8 suppresses HL-60 cell apoptosis [46]. The expression of S100A8 may vary in different organ tumors, different types of tumors in the same organ, or even at different stages of development of the same tumor, indicating that it has a dual role [18]. Previous studies have demonstrated that S100A8 is pro-migratory at lower concentrations [47], but pro-apoptotic at higher concentrations [48]. In addition, research has confirmed the existence of a balance between anti-carcinogenicity and carcinogenicity of S100A8, but how the balance is tipped depends on the expression level and location of S100A8 [49].

Many studies have shown that S100A8 is associated with signaling pathways in various cancer cells [30,50]. In OC cells, several pathways related to cell proliferation, migration, apoptosis, and invasion are involved, including the Wnt/β-catenin [51,52], mTOR [53], and extracellular signal-regulated kinase (ERK) signaling pathways [54]. S100A8 promoted the survival and migration of colon cancer cells through activation of the Wnt/β-catenin pathway [15]. In uroepithelial carcinoma, activation of the NF-κB pathway by S100A8 blocked apoptosis [55]. As the impacts of S1000A8 on autophagy and apoptosis in OC cells mediated through the PI3K/Akt pathway and the critical role of the PI3K/Akt pathway in regulating cell proliferation, survival, autophagy, and apoptosis remain under-explored, in this study, we aimed to investigate, depending on the activation status of PI3K/Akt signaling pathway, the influence of S100A8 on autophagy and apoptosis in OC cells. Additionally, this pathway is implicated in several pathological conditions, including a range of tumor types [56,57]. Research has shown that the PI3K/Akt pathway is involved in the autophagy and apoptosis of OC cells [58,59]. Knockdown of S100A8 has been reported to enhance cell proliferation and trigger breast cancer through the PI3K/Akt signaling pathway [32]. In the current study, our results showed that PI3K/Akt activation using 1,5-DQA blocked the inhibitory effects of S100A8 on OC cell activity, autophagy and migration, and its promotion of apoptosis, indicating that inhibition of the PI3K/Akt pathway is the mechanism through which S100A8 induces apoptosis and suppresses proliferation, autophagy and migration of OC cells.

Conclusions

In summary, S100A8 inhibits proliferation, migration and autophagy, and promotes apoptosis in ovarian cancer cells by inhibiting the PI3K/Akt pathway. Thus, S100A8 holds promise as a potential target for the prevention and treatment of ovarian cancer, providing an effective therapeutic strategy for the clinic.

Availability of Data and Materials

Data and materials from this study can be obtained from the corresponding author upon reasonable request.

Author Contributions

XJM and GYC designed the research study and wrote the first draft. XJM and YW performed the research. XJM, YW and GYC analyzed the data. All authors were involved in the critical revision of the manuscript. All authors read and approved the final manuscript. All authors have participated sufficiently in the work and agreed to be accountable for all aspects of the work.

Ethics Approval and Consent to Participate

Not applicable.

Acknowledgment

Not applicable.

Funding

This research received no external funding.

Conflict of Interest

The authors declare no conflict of interest.

References

[1] Tajmul M, Parween F, Singh L, Mathur SR, Sharma JB, Kumar S, *et al*. Identification and validation of salivary proteomic signatures for non-invasive detection of ovarian cancer. International Journal of Biological Macromolecules. 2018; 108: 503–514. https://doi.org/10.1016/j.ijbiomac.2017.12.014.

[2] Bai Y, Li LD, Li J, Lu X. Prognostic values of S100 family members in ovarian cancer patients. BMC Cancer. 2018; 18: 1256. https://doi.org/10.1186/s12885-018-5170-3.

[3] Clarke-Pearson DL. Clinical practice. Screening for ovarian cancer. The New England Journal of Medicine. 2009; 361: 170–177. https://doi.org/10.1056/NEJMcp0901926.

[4] Kim SJ, Rosen B, Fan I, Ivanova A, McLaughlin JR, Risch H, *et al*. Epidemiologic factors that predict long-term survival following a diagnosis of epithelial ovarian cancer. British Journal of Cancer. 2017; 116: 964–971. https://doi.org/10.1038/bjc.2017.35.

[5] Grossman DC, Curry SJ, Owens DK, Barry MJ, Davidson KW, Doubeni CA, *et al*. Screening for ovarian cancer: US preventive services task force recommendation statement. JAMA. 2018; 319: 588–594. https://doi.org/10.1001/jama.2017.21926.

[6] Zimmer DB, Cornwall EH, Landar A, Song W. The S100 protein family: history, function, and expression. Brain Research Bulletin. 1995; 37: 417–429. https://doi.org/10.1016/0361-9230(95)00040-2.

[7] Donato R. S100: a multigenic family of calcium-modulated proteins of the EF-hand type with intracellular and extracellular functional roles. The International Journal of Biochemistry & Cell Biology. 2001; 33: 637–668. https://doi.org/10.1016/s1357-2725(01)00046-2.

[8] Heizmann CW, Fritz G, Schäfer BW. S100 proteins: structure, functions and pathology. Frontiers in Bioscience: a Journal and Virtual Library. 2002; 7: d1356–68. https://doi.org/10.2741/A846.

[9] Fujita Y, Khateb A, Li Y, Tinoco R, Zhang T, Bar-Yoseph H, *et al*. Regulation of S100A8 Stability by RNF5 in Intestinal Epithelial Cells Determines Intestinal Inflammation and Severity of Colitis. Cell Reports. 2018; 24: 3296–3311.e6. https://doi.org/10.1016/j.celrep.2018.08.057.

[10] Hermani A, Hess J, De Servi B, Medunjanin S, Grobholz R, Trojan L, *et al*. Calcium-binding proteins S100A8 and S100A9 as novel diagnostic markers in human prostate cancer. Clinical Cancer Research: an Official Journal of the American Association for Cancer Research. 2005; 11: 5146–5152. https://doi.org/10.1158/1078-0432.CCR-05-0352.

[11] Gebhardt C, Németh J, Angel P, Hess J. S100A8 and S100A9 in inflammation and cancer. Biochemical Pharmacology. 2006; 72: 1622–1631. https://doi.org/10.1016/j.bcp.2006.05.017.

[12] Huang A, Fan W, Liu J, Huang B, Cheng Q, Wang P, *et al*. Prognostic Role of S100A8 in Human Solid Cancers: A Systematic Review and Validation. Frontiers in Oncology. 2020; 10: 564248. https://doi.org/10.3389/fonc.2020.564248.

[13] Wen L, Ding Y, Chen X, Tian K, Li D, Liang K, *et al*. Influences of S100A8 and S100A9 on Proliferation of Nasopharyngeal Carcinoma Cells through PI3K/Akt Signaling Pathway. BioMed Research International. 2021; 2021: 9917365. https://doi.org/10.1155/2021/9917365.

[14] Tanigawa K, Tsukamoto S, Koma YI, Kitamura Y, Urakami S, Shimizu M, *et al*. S100A8/A9 Induced by Interaction with Macrophages in Esophageal Squamous Cell Carcinoma Promotes the Migration and Invasion of Cancer Cells via Akt and p38 MAPK Pathways. The American Journal of Pathology. 2022; 192: 536–552. https://doi.org/10.1016/j.ajpath.2021.12.002.

[15] Duan L, Wu R, Ye L, Wang H, Yang X, Zhang Y, *et al*. S100A8 and S100A9 are associated with colorectal carcinoma progression and contribute to colorectal carcinoma cell survival and migration via Wnt/β-catenin pathway. PloS One. 2013; 8: e62092. https://doi.org/10.1371/journal.pone.0062092.

[16] Kwon CH, Moon HJ, Park HJ, Choi JH, Park DY. S100A8 and S100A9 promotes invasion and migration through p38 mitogen-activated protein kinase-dependent NF-κB activation in gastric cancer cells. Molecules and Cells. 2013; 35: 226–234. https://doi.org/10.1007/s10059-013-2269-x.

[17] Zhang Y, Zha Z, Shen W, Li D, Kang N, Chen Z, *et al*. Anemoside B4 ameliorates TNBS-induced colitis through S100A9/MAPK/NF-κB signaling pathway. Chinese Medicine. 2021; 16: 11. https://doi.org/10.1186/s13020-020-00410-1.

[18] Srikrishna G. S100A8 and S100A9: new insights into their roles in malignancy. Journal of Innate Immunity. 2012; 4: 31–40. https://doi.org/10.1159/000330095.

[19] Teng Z, Wang C, Wang Y, Huang K, Xiang X, Niu W, *et al*. S100A8, An Oocyte-Specific Chemokine, Directs the Migration of Ovarian Somatic Cells During Mouse Primordial Follicle Assembly. Journal of Cellular Physiology. 2015; 230: 2998–3008. https://doi.org/10.1002/jcp.25032.

[20] Robbins HL, Hague A. The PI3K/Akt Pathway in Tumors of Endocrine Tissues. Frontiers in Endocrinology. 2016; 6: 188. https://doi.org/10.3389/fendo.2015.00188.

[21] Jiang H, Gao M, Shen Z, Luo B, Li R, Jiang X, *et al*. Blocking PI3K/Akt signaling attenuates metastasis of nasopharyngeal carcinoma cells through induction of mesenchymal-epithelial reverting transition. Oncology Reports. 2014; 32: 559–566. https://doi.org/10.3892/or.2014.3220.

[22] Saji M, Vasko V, Kada F, Allbritton EH, Burman KD, Ringel MD. Akt1 contains a functional leucine-rich nuclear export sequence. Biochemical and Biophysical Research Communications. 2005; 332: 167–173. https://doi.org/10.1016/j.bbrc.2005.04.109.

[23] Hers I, Vincent EE, Tavaré JM. Akt signalling in health and disease. Cellular Signalling. 2011; 23: 1515–1527. https://doi.org/10.1016/j.cellsig.2011.05.004.

[24] Martelli AM, Tabellini G, Bressanin D, Ognibene A, Goto K, Cocco L, *et al*. The emerging multiple roles of nuclear Akt. Biochimica et Biophysica Acta. 2012; 1823: 2168–2178. https://doi.org/10.1016/j.bbamcr.2012.08.017.

[25] Li A, Gu Y, Li X, Sun H, Zha H, Xie J, *et al*. S100A6 promotes the proliferation and migration of cervical cancer cells via the PI3K/Akt signaling pathway. Oncology Letters. 2018; 15: 5685–5693. https://doi.org/10.3892/ol.2018.8018.

[26] Yi W, Zhu R, Hou X, Wu F, Feng R. Integrated Analysis Reveals S100a8/a9 Regulates Autophagy and Apoptosis through the MAPK and PI3K-AKT Signaling Pathway in the Early Stage

of Myocardial Infarction. Cells. 2022; 11: 1911. https://doi.org/10.3390/cells11121911.

[27] Ocana A, Vera-Badillo F, Al-Mubarak M, Templeton AJ, Corrales-Sanchez V, Diez-Gonzalez L, *et al*. Activation of the PI3K/mTOR/AKT pathway and survival in solid tumors: systematic review and meta-analysis. PloS One. 2014; 9: e95219. https://doi.org/10.1371/journal.pone.0095219.

[28] Xiao HB, Cao X, Wang L, Run XQ, Su Y, Tian C, *et al*. 1,5-dicaffeoylquinic acid protects primary neurons from amyloid β 1-42-induced apoptosis via PI3K/Akt signaling pathway. Chinese Medical Journal. 2011; 124: 2628–2635.

[29] Li F, Hu J, Tian J, Xu K, Ni M, Wang B, *et al*. Effects of phoxim on nutrient metabolism and insulin signaling pathway in silkworm midgut. Chemosphere. 2016; 146: 478–485. https://doi.org/10.1016/j.chemosphere.2015.12.032.

[30] Reeb AN, Li W, Sewell W, Marlow LA, Tun HW, Smallridge RC, *et al*. S100A8 is a novel therapeutic target for anaplastic thyroid carcinoma. The Journal of Clinical Endocrinology and Metabolism. 2015; 100: E232–42. https://doi.org/10.1210/jc.2014-2988.

[31] Si X, Xu F, Xu F, Wei M, Ge Y, Chenge S. CADM1 inhibits ovarian cancer cell proliferation and migration by potentially regulating the PI3K/Akt/mTOR pathway. Biomedicine & Pharmacotherapy = Biomedecine & Pharmacotherapie. 2020; 123: 109717. https://doi.org/10.1016/j.biopha.2019.109717.

[32] Singh P, Ali SA, Kumar S, Mohanty AK. CRISPR-Cas9 based knockout of S100A8 in mammary epithelial cells enhances cell proliferation and triggers oncogenic transformation via the PI3K-Akt pathway: Insights from a deep proteomic analysis. Journal of Proteomics. 2023; 288: 104981. https://doi.org/10.1016/j.jprot.2023.104981.

[33] Dimova I, Orsetti B, Theillet C, Dimitrov R, Toncheva D. Copy number changes in 1q21. 3 and 1q23. 3 have different clinical relevance in ovarian tumors. Balkan Journal of Medical Genetics. 2009; 12: 29–37. https://doi.org/10.2478/v10034-010-0009-5.

[34] Wang D, Liu G, Wu B, Chen L, Zeng L, Pan Y. Clinical Significance of Elevated S100A8 Expression in Breast Cancer Patients. Frontiers in Oncology. 2018; 8: 496. https://doi.org/10.3389/fonc.2018.00496.

[35] Li S, Zhang J, Qian S, Wu X, Sun L, Ling T, *et al*. S100A8 promotes epithelial-mesenchymal transition and metastasis under TGF-β/USF2 axis in colorectal cancer. Cancer Communications (London, England). 2021; 41: 154–170. https://doi.org/10.1002/cac2.12130.

[36] Mirza Z, Schulten HJ, Farsi HM, Al-Maghrabi JA, Gari MA, Chaudhary AG, *et al*. Impact of S100A8 expression on kidney cancer progression and molecular docking studies for kidney cancer therapeutics. Anticancer Research. 2014; 34: 1873–1884.

[37] Ghavami S, Chitayat S, Hashemi M, Eshraghi M, Chazin WJ, Halayko AJ, *et al*. S100A8/A9: a Janus-faced molecule in cancer therapy and tumorgenesis. European Journal of Pharmacology. 2009; 625: 73–83. https://doi.org/10.1016/j.ejphar.2009.08.044.

[38] Motley AM, Nuttall JM, Hettema EH. Pex3-anchored Atg36 tags peroxisomes for degradation in Saccharomyces cerevisiae. The EMBO Journal. 2012; 31: 2852–2868. https://doi.org/10.1038/emboj.2012.151.

[39] Das S, Shukla N, Singh SS, Kushwaha S, Shrivastava R. Mechanism of interaction between autophagy and apoptosis in cancer. Apoptosis: an International Journal on Programmed Cell Death. 2021; 26: 512–533. https://doi.org/10.1007/s10495-021-01687-9.

[40] Sun Y, Liu JH, Jin L, Lin SM, Yang Y, Sui YX, *et al*. Overexpression of the Beclin1 gene upregulates chemosensitivity to anti-cancer drugs by enhancing therapy-induced apoptosis in cervix squamous carcinoma CaSki cells. Cancer Letters. 2010; 294: 204–210. https://doi.org/10.1016/j.canlet.2010.02.001.

[41] Sun Y, Liu JH, Pan L, Jin L, Yang Y, Sui YX, *et al*. Modulatory effects of Beclin 1 on expression of angiopoietin and Tie-2 receptor in human cervical cancer cells. Asian Pacific Journal of Cancer Prevention: APJCP. 2011; 12: 2985–2990.

[42] Kabeya Y, Mizushima N, Ueno T, Yamamoto A, Kirisako T, Noda T, *et al*. LC3, a mammalian homologue of yeast Apg8p, is localized in autophagosome membranes after processing. The EMBO Journal. 2000; 19: 5720–5728. https://doi.org/10.1093/emboj/19.21.5720.

[43] Cheng HY, Zhang YN, Wu QL, Sun XM, Sun JR, Huang X. Expression of beclin 1, an autophagy-related protein, in human cervical carcinoma and its clinical significance. European Journal of Gynaecological Oncology. 2012; 33: 15–20.

[44] Fujii S, Mitsunaga S, Yamazaki M, Hasebe T, Ishii G, Kojima M, *et al*. Autophagy is activated in pancreatic cancer cells and correlates with poor patient outcome. Cancer Science. 2008; 99: 1813–1819. https://doi.org/10.1111/j.1349-7006.2008.00893.x.

[45] Li Y, Hu P, Zhang Z, Yuan Z, Yang K, Sun Z. Protective autophagy alleviates neurotoxin-gelsenicine induced apoptosis through PERK signaling pathway in Neuro-2a cells. Toxicology. 2022; 474: 153210. https://doi.org/10.1016/j.tox.2022.153210.

[46] Yang XY, Zhang MY, Zhou Q, Wu SY, Zhao Y, Gu WY, *et al*. High expression of S100A8 gene is associated with drug resistance to etoposide and poor prognosis in acute myeloid leukemia through influencing the apoptosis pathway. OncoTargets and Therapy. 2016; 9: 4887–4899. https://doi.org/10.2147/OTT.S101594.

[47] Iotzova-Weiss G, Dziunycz PJ, Freiberger SN, Läuchli S, Hafner J, Vogl T, *et al*. S100A8/A9 stimulates keratinocyte proliferation in the development of squamous cell carcinoma of the skin via the receptor for advanced glycation-end products. PloS One. 2015; 10: e0120971. https://doi.org/10.1371/journal.pone.0120971.

[48] Ghavami S, Eshragi M, Ande SR, Chazin WJ, Klonisch T, Halayko AJ, *et al*. S100A8/A9 induces autophagy and apoptosis via ROS-mediated cross-talk between mitochondria and lysosomes that involves BNIP3. Cell Research. 2010; 20: 314–331. https://doi.org/10.1038/cr.2009.129.

[49] Narumi K, Miyakawa R, Ueda R, Hashimoto H, Yamamoto Y, Yoshida T, *et al*. Proinflammatory Proteins S100A8/S100A9 Activate NK Cells via Interaction with RAGE. Journal of Immunology (Baltimore, Md.: 1950). 2015; 194: 5539–5548. https://doi.org/10.4049/jimmunol.1402301.

[50] Pan S, Hu Y, Hu M, Xu Y, Chen M, Du C, *et al*. S100A8 facilitates cholangiocarcinoma metastasis via upregulation of VEGF through TLR4/NF κB pathway activation. International Journal of Oncology. 2020; 56: 101–112. https://doi.org/10.3892/ijo.2019.4907.

[51] Nagaraj AB, Joseph P, Kovalenko O, Singh S, Armstrong A, Redline R, *et al*. Critical role of Wnt/β-catenin signaling in driving epithelial ovarian cancer platinum resistance. Oncotarget. 2015; 6: 23720–23734. https://doi.org/10.18632/oncotarget.4690.

[52] Guo C, Wang X, Chen LP, Li M, Li M, Hu YH, *et al*. Long non-coding RNA MALAT1 regulates ovarian cancer cell proliferation, migration and apoptosis through Wnt/β-catenin signaling pathway. European Review for Medical and Pharmacological Sciences. 2018; 22: 3703–3712. https://doi.org/10.26355/eurrev_201806_15249.

[53] Zhou H, Zhao H, Liu H, Xu X, Dong X, Zhao E. Influence of carboplatin on the proliferation and apoptosis of ovarian cancer cells through mTOR/p70s6k signaling pathway. Journal of B.U.ON.: Official Journal of the Balkan Union of Oncology.

2018; 23: 1732–1738.

[54] Liu SB, Lin XP, Xu Y, Shen ZF, Pan WW. DAXX promotes ovarian cancer ascites cell proliferation and migration by activating the ERK signaling pathway. Journal of Ovarian Research. 2018; 11: 90. https://doi.org/10.1186/s13048-018-0462-4.

[55] Lyu ZJ, Wang Y, Huang JL, Chen M, Wu SY, Yan Q, *et al*. Recurrent ZNF83-E293V Mutation Promotes Bladder Cancer Progression through the NF-κB Pathway via Transcriptional Dysregulation of S100A8. Molecular Therapy: the Journal of the American Society of Gene Therapy. 2021; 29: 275–290. https://doi.org/10.1016/j.ymthe.2020.09.004.

[56] Yang SX, Polley E, Lipkowitz S. New insights on PI3K/AKT pathway alterations and clinical outcomes in breast cancer. Cancer Treatment Reviews. 2016; 45: 87–96. https://doi.org/10.1016/j.ctrv.2016.03.004.

[57] Xu Z, Han X, Ou D, Liu T, Li Z, Jiang G, *et al*. Targeting PI3K/AKT/mTOR-mediated autophagy for tumor therapy. Applied Microbiology and Biotechnology. 2020; 104: 575–587. https://doi.org/10.1007/s00253-019-10257-8.

[58] Cai Y, Tan X, Liu J, Shen Y, Wu D, Ren M, *et al*. Inhibition of PI3K/Akt/mTOR signaling pathway enhances the sensitivity of the SKOV3/DDP ovarian cancer cell line to cisplatin in vitro. Chinese Journal of Cancer Research = Chung-kuo Yen Cheng Yen Chiu. 2014; 26: 564–572. https://doi.org/10.3978/j.issn.1000-9604.2014.08.20.

[59] Westfall SD, Skinner MK. Inhibition of phosphatidylinositol 3-kinase sensitizes ovarian cancer cells to carboplatin and allows adjunct chemotherapy treatment. Molecular Cancer Therapeutics. 2005; 4: 1764–1771. https://doi.org/10.1158/1535-7163.MCT-05-0192.